



**AIAA 2001-2138**

**The Detection of Radiated Modes From  
Ducted Fan Engines**

F. Farassat, Douglas M. Nark, and Russell  
H. Thomas  
NASA Langley Research Center  
Hampton, VA 23681

**7th AIAA/CEAS  
Aeroacoustics Conference**

**May 28-30, 2001  
Maastricht, The Netherlands**



# The Detection of Radiated Modes From Ducted Fan Engines

F. Farassat,\* Douglas M. Nark,† and Russell H. Thomas‡  
NASA Langley Research Center  
Hampton, VA 23681

## Abstract

The bypass duct of an aircraft engine is a low-pass filter allowing some spinning modes to radiate outside the duct. The knowledge of the radiated modes can help in noise reduction, as well as the diagnosis of noise generation mechanisms inside the duct. We propose a nonintrusive technique using a circular microphone array outside the engine measuring the complex noise spectrum on an arc of a circle. The array is placed at various axial distances from the inlet or the exhaust of the engine. Using a model of noise radiation from the duct, an overdetermined system of linear equations is constructed for the complex amplitudes of the radial modes for a fixed circumferential mode. This system of linear equations is generally singular, indicating that the problem is ill-posed. Tikhonov regularization is employed to solve this system of equations for the unknown amplitudes of the radiated modes. An application of our mode detection technique using measured acoustic data from a circular microphone array is presented. We show that this technique can reliably detect radiated modes with the possible exception of modes very close to cut-off.

\*Senior Research Scientist, Aeroacoustics Branch, Aerodynamics, Aerothermodynamics and Acoustics Competency, AIAA Associate Fellow

†Computer Sciences Corporation, AIAA Member

‡Research Scientist, Aeroacoustics Branch, Aerodynamics, Aerothermodynamics and Acoustics Competency, AIAA Senior Member

Copyright ©2001 by the American Institute of Aeronautics and Astronautics, Inc. No copyright is asserted in the United States under Title 17, U.S. Code. The U.S. Government has a royalty-free license to exercise all rights under the copyright claimed herein for government purposes. All other rights are reserved by the copyright owner.

## List of Symbols

$a$	radius of circular microphone array
$A(\psi, \theta')$	a complex function defined in equation (17)
$A_q$	the vector $(A_{q1}, A_{q2}, \dots, A_{qn})^T$
$A_{qn}$	amplitude of mode $(m, n)$ , $m = \alpha B + qV$
$B$	fan blade number
BPF	blade passage frequency $(B\Omega/2\pi)$
$c$	speed of sound
$C(m, n, \psi)$	a parameter defined in equation (12)
$d_q$	the vector $(D_q(\psi_1), D_q(\psi_2), \dots, D_q(\psi_j))^T$
$D_q$	a parameter defined in equation (16)
$f$	frequency
$\mathbf{G}$	a $j \times n$ matrix, $j \geq n$ , see equation (23)
$\mathbf{G}^*$	the Hermitian adjoint of $\mathbf{G}$
$G$	the linear operator mapping $X$ into $Y$ whose matrix is $\mathbf{G}$
$g_{vw}$	element of the matrix $\mathbf{G}$
$J_m(x)$	Bessel function of first kind and order $m$
$k$	wavenumber, $\alpha B\Omega/c$
$k_a(m, n)$	axial wavenumber of mode $(m, n)$ , see equation (22)
$k_r(m, n)$	radial wavenumber of mode $(m, n)$ , see equation (19)
$m$	circumferential mode number
$M$	duct Mach number, $M < 0$ for inlet radiation
$n$	radial mode number, $n = 1, 2, \dots$
$N_G$	the nullspace of linear operator $G$
$p'(\vec{x}, t)$	acoustic pressure
$\hat{p}'(\vec{x}, f)$	temporal Fourier transform of $p'(\vec{x}, t)$
$P(\vec{x}, \alpha B\Omega)$	see equation (14)
$\hat{P}_q$	Fourier transform of $P$ in azimuthal variable $\theta'$ , see equation (15)
$q$	a parameter defining circumferential mode $m$ in the relation $m = \alpha B + qV$ , $q = 0, \pm 1, \pm 2, \dots$

$r$	radial coordinate of a point on the duct inlet or exhaust surface, see figure (2)
$r_0$	duct radius
$R_G$	the range of linear operator $G$
$R_0$	distance of a microphone from the duct inlet or exhaust center
$\bar{R}$	distance between a microphone and a point on the the inlet or exhaust surface
ret	as a subscript, retarded time
$s$	the dimension of the range of $G$
$S$	in $dS$ , surface area
SVD	Singular Value Decomposition
$t$	time
$T$	as a subscript, Tikhonov
$u$	axial velocity of the sound wave
$u_i$	basis vectors in the subspace $X \setminus N_G$ , $i = 1, 2, \dots, s$
$v_i$	basis vectors in $R_G$ , $i = 1, 2, \dots, s$
$V$	number of vanes in stator, number of circumferentially symmetric disturbances interacting with the rotor blades
$x$	axial distance from inlet or exhaust center
$X$	the $n$ -dimensional linear space where the solution vector $A_q$ is sought
$Y$	the $j$ -dimensional linear space where the vector $d_q$ lies

#### Greek Symbols:

$\alpha$	multiple of BPF
$\alpha_T$	Tikhonov parameter
$\beta$	$\sqrt{1 - M^2}$
$\theta$	angular coordinate of a point on the inlet or exhaust surface in cylindrical polar coordinates, see figure (2)
$\theta'$	angular coordinate of a microphone in cylindrical polar coordinates, see figure (2)
$\xi(m, n)$	cut-off ratio, see equation (20)
$\mu_i$	singular values of matrix $\mathbf{G}$ , $i = 1, 2, \dots, n$ , $\mu_i^2$ are the eigenvalues of $\mathbf{G}^* \mathbf{G}$ , $\mu_i \geq 0$
$\rho_0$	density of air in the exterior region of the duct
$\psi$	angle that the line joining a microphone to the center of the duct inlet or exhaust makes with the $x$ -axis
$\Omega$	angular velocity of the rotor

#### Other Symbols:

$\ \cdot\ $	$L_1, L_2$ , or $L_\infty$ norm of a vector
-------------	---

$\cdot \setminus \cdot$	as in $X \setminus N_R$ , set subtraction
$\langle \cdot, \cdot \rangle$	complex inner product.

## 1. Introduction

The detection of the radiated modes from an aircraft engine can help in the diagnosis of noise generation mechanisms inside the duct and provide guidance for noise control. A duct is a low-pass filter that allows some of the spinning modes inside the duct to escape outside. In general, each radiated mode has a specific directivity pattern. The combined interference of all the radiated modes results in a complicated spatial pattern that rotates at the engine speed. The problem of the discovery of any information about the radiated modes is known as an *inverse problem*. The study of inverse problems is currently an active area of research. These problems appear in many areas of science, engineering, and medicine. For example, magnetic resonance imaging (MRI) in medicine, which allows physicians to obtain images of the internal organs of patients, can be classified as an inverse problem. Other examples appear in oil and mineral prospecting, seismology, and satellite imaging.

One method of mode detection was proposed by Pickett *et al.* in the mid-Seventies.<sup>1</sup> It uses a microphone rake rotating at steady speed in the duct inlet or exhaust. This method was successfully implemented by Heidelberg and coworkers who designed a microphone rake rotating at a fraction of the engine speed.<sup>2</sup> The rotating rig size is dependent on engine size, requiring sophisticated mechanical and electronic components. In addition, the wake from the rake may interact with fan blades if used in the inlet. The resulting interaction noise can be separated from the engine noise in most cases, but may complicate the interpretation of the results. We present another method which employs a circular microphone array outside the engine and, thus, is nonintrusive. The associated measurement rig can be used for a range of engine sizes. In addition, the microphone rig is very simple, using some stepping motors to move the microphones (located on a circular arc) circumferentially and axially.

We employ Rayleigh's piston in a wall formula to model the radiation from the inlet or exhaust plane of the duct. For each multiple of the blade passage frequency (BPF), the complex temporal Fourier transform of the acoustic pressure is first obtained over an arc of a circle at a fixed axial distance from the duct lip. The Fourier decomposition in the az-

imuthal direction of the temporal transform can then be related to the amplitudes of the radiated modes at the duct inlet or exhaust. For a given circumferential  $m$ , a single linear equation is obtained in terms of the amplitudes of the radial modes which propagate outside the duct. Repeating this calculation for several axial distances, a set of simultaneous linear equations for the amplitudes of the radial modes for the circumferential mode  $m$  is obtained. In principle, this system of linear equations can be solved to get the amplitudes of the radial modes. There are, however, some problems. For a given circumferential mode, the number of radial modes that will propagate outside of the duct is not known. Therefore, we propose to take more axial measurements than is necessary (*i.e.* we work with an overdetermined system of equations). Furthermore, the problem is ill-posed and techniques for extracting the proper information from the linear equations must be employed. We use the Tikhonov regularization technique which is a well known method of dealing with ill-posed problems.<sup>3,4</sup>

In Section 2, we present the detailed mathematical derivation behind the mode detection technique. There are practical problems in finding the phase of the complex temporal Fourier transform of the acoustic field for a multiple of the BPF because we can not measure sound simultaneously at all points of the space. This necessitates the use of a reference microphone and the cross spectrum to extract the phase information. In Section 3, we discuss the ill-posedness of the problem and how we remedy this problem by regularization. Results from an experiment on a 12 inch diameter model are presented in Section 4. The calculations show that our mode detection method works well for modes that are not very close to the cut-off condition. Finally, concluding remarks follow in Section 5.

## 2. Mode Detection Theory

In this section, the mathematical theory of the mode detection, which was originally discussed by Farassat and Myers<sup>5</sup> is presented. Figure 1 shows the circular microphone array (CMA) of radius  $a$  at a distance  $x$  from the duct, radius  $r_0$ , inlet (or exhaust). The microphone array plane is parallel to the duct inlet plane and the center of the array circle lies on the extension of the duct axis as shown in figure 1. It is assumed that we have a uniform flow with the Mach number  $M$  inside the duct. Since the positive  $x$ -axis points out of the duct,  $M < 0$  for the inlet and  $M > 0$  for the exhaust noise study.

The number of blades of the rotor is  $B$  and  $\Omega$  is the shaft angular frequency. The blade passage frequency (BPF) is, therefore,  $B\Omega/2\pi$ . The number of stator vanes is  $V$ , which can also be assumed to be the number of axially symmetric disturbances interacting with the rotor. The circumferential mode numbers,  $m$ , due to rotor-stator interaction are given by the relation

$$m = \alpha B + qV \quad q = 0, \pm 1, \pm 2, \dots \quad (1)$$

where  $\alpha$  is the multiple of BPF. For a given  $\alpha$ , we note that  $q$  specifies  $m$ , *i.e.*  $m = m(q)$ . In what follows, we find that it is convenient to work with  $q$  rather than  $m$ . Our aim is to obtain a system of simultaneous linear equations for the radial modes associated with a fixed  $\alpha$  and  $q$  that radiate outside the duct. Although we refer to duct inlet noise radiation, the analysis is also valid for duct exhaust with the appropriate duct Mach number,  $M$ , axial wave number,  $k_a$ , and radial wave number,  $k_r$ .

We use Rayleigh's piston in the wall formula as the model of noise radiation from the inlet

$$4\pi p'(\vec{x}, t) = \int_{\text{inlet area}} \frac{\rho_0 [\dot{u}]_{\text{ret}}}{\bar{R}} dS \quad (2)$$

where  $u(r, \theta, 0, t)$  is the fluctuating axial velocity of the sound wave at the inlet,  $x = 0$ , and  $\bar{R}$  is the radiation distance as shown in figure 2. The origin of the cylindrical polar coordinate  $(r, \theta, x)$  is at the center of the duct inlet with the microphone coordinates at  $(a, \theta', x)$ . The acoustic pressure in the duct is described by

$$p'(r, \theta, x, t) = e^{i\alpha B(\Omega t - \theta)} \times \sum_n \sum_q A_{qn} J_m [k_r(m, n)r] e^{-i[qV\theta + k_a(m, n)x]} \quad (3)$$

where  $J_m(\cdot)$  is the Bessel function of the first kind of order  $m$ ,  $k_a$  is the axial wave number, and  $k_r$  is the radial wave number. Note that both  $k_a$  and  $k_r$  are functions of the circumferential mode number  $m$  and radial mode number  $n$ . In equation (3),  $A_{qn}$  is the amplitude of the mode  $(m, n)$  (*i.e.*  $A_{qn}$  stands for  $A_{mn}$ ). We are summing over  $q$  in this equation and  $m = \alpha B + qV = m(q)$  everywhere.

The relation between  $p'(m, n)$  and  $u(m, n)$  is found from the linearized momentum equation as

$$u(m, n) = \frac{k_a(m, n)p'(m, n)}{\alpha B\Omega\rho_0} \quad (4)$$

Using this equation and equation (3), the axial velocity of sound at the inlet,  $x = 0$ , is

$$u(r, \theta, 0, t) = \frac{1}{\alpha B \Omega \rho_0} e^{i\alpha B(\Omega t - \theta)} \times \sum_n \sum_q A_{qn} k_a(m, n) J_m[k_a(m, n)r] e^{-iqV\theta} \quad (5)$$

which simply gives

$$\dot{u}(r, \theta, 0, t) = i\alpha B \Omega u(r, \theta, 0, t) \quad (6)$$

Next, we assume that the duct radius  $r_0$  satisfies  $r_0 \ll R_0$  where  $R_0$  is the distance from a microphone on the array to the duct inlet center. Then, since  $r \leq r_0$ , we can show that

$$\tilde{R} \approx R_0 - r \sin \psi \cos(\theta - \theta') \quad (7)$$

where  $\sin \psi = a/R_0$  and  $\psi$  is the angle that the line joining a microphone to the duct inlet center makes with the  $x$ -axis (see figure 2). From equations (5-7), we obtain

$$[\dot{u}]_{\text{ret}} = \frac{i}{\rho_0} e^{i\alpha B[\Omega(t - R_0/c) - \theta']} \times \sum_n \sum_q e^{-iqV\theta'} A_{qn} k_a J_m(k_r r) \times e^{i[kr \sin \psi \cos(\theta - \theta') - m(\theta - \theta')]} \quad (8)$$

where  $k = \alpha B \Omega / c$  and  $k_a$  and  $k_r$  are functions of  $(m, n)$ .

We can write the surface integral in equation (2) as follows:

$$\int_{\text{inlet area}} \dots dS = \int_0^{r_0} r dr \int_0^{2\pi} \dots d\theta \quad (9)$$

Using the approximation  $\tilde{R} \approx R_0$  in the denominator of equation (2), the only term in  $[\dot{u}]_{\text{ret}}$  dependent on the angle  $\theta$  is the last exponential function in the summation in equation (8). This term can be integrated analytically in the variable  $\theta$  as follows:

$$\int_0^{2\pi} e^{i[kr \sin \psi \cos(\theta - \theta') - m(\theta - \theta')]} d\theta = 2\pi e^{im\pi/2} J_m(kr \sin \psi) \quad (10)$$

The acoustic pressure at the microphone location  $\vec{x} = (a, \theta', x)$  is thus given, from equation (2), as

$$p'(\vec{x}, t) = \frac{i}{2R_0} e^{i\alpha B[\Omega(t - R_0/c) - \theta' + \pi/2]} \times \sum_n \sum_q C(m, n, \psi) A_{qn} k_a(m, n) e^{-iqV(\theta' - \pi/2)} \quad (11)$$

where

$$C(m, n, \psi) = \int_0^{r_0} r J_m\left(\frac{\alpha B \Omega r}{c} \sin \psi\right) J_m[k_r(m, n)] dr \quad (12)$$

Our mode detection technique is based on equation (11) which we will discuss below.

The complex temporal Fourier transform of  $p'(\vec{x}, t)$  at a frequency of  $\alpha$  times BPF is

$$\hat{p}'(\vec{x}, \alpha B \Omega) = \frac{i}{2R_0} e^{-i\alpha B(\Omega R_0/c + \theta' - \pi/2)} \times \sum_n \sum_q C(m, n, \psi) A_{qn} k_a(m, n) e^{-iqV(\theta' - \pi/2)} \quad (13)$$

Let us now define

$$\begin{aligned} P(\vec{x}, \alpha B \Omega) &= -2iR_0 e^{i\alpha B(\Omega R_0/c + \theta' - \pi/2)} \hat{p}'(\vec{x}, \alpha B \Omega) \quad (14) \\ &= \sum_n \sum_q C(m, n, \psi) A_{qn} k_a(m, n) e^{-iqV(\theta' - \pi/2)} \end{aligned}$$

If we find  $P(\vec{x}, \alpha B \Omega)$  for  $0 \leq \theta' \leq \pi$ , then the complex Fourier Transform of  $P$  in the azimuthal direction,  $\theta'$  gives

$$\begin{aligned} \hat{P}_q &\equiv \frac{1}{\pi} \int_0^\pi P(\vec{x}, \alpha B \Omega) e^{iqV\theta'} d\theta' \quad (15) \\ &= e^{iqV\pi/2} \sum_n [C(m, n, \psi) k_a(m, n)] A_{qn}. \end{aligned}$$

From this result, we find

$$\begin{aligned} D_q &\equiv e^{-iqV\pi/2} \hat{P}_q \quad (16) \\ &= \sum_n [C(m, n, \psi) k_a(m, n)] A_{qn}. \end{aligned}$$

This is a linear equation for the amplitudes of all radial modes associated with a fixed circumferential mode,  $m = \alpha B + qV$ , that radiate outside the duct. Each axial position of the array supplies one linear equation for  $A_{qn}$ . Measuring the noise radiated from the duct at many axial locations gives an overdetermined system of linear equations for the known  $A_{qn}$  ( $q$  fixed) for the associated radial modes. One then solves this system of linear equations to get the radial mode amplitudes  $A_{qn}$ .

## Remarks

1. Equation (11) shows that the acoustic field of the noise radiated from the duct may be represented in the far field as

$$p'(\vec{x}, t) = \frac{e^{-ikR_0}}{R_0} A(\psi, \theta') e^{i\alpha B(\Omega t - \theta')} \quad (17)$$

where  $A(\psi, \theta')$  is a complex function which is periodic in the azimuthal angle,  $\theta'$  with periodicity  $2\pi/V$ . This result indicates that the information about  $A_{qn}$  is hidden in  $A(\psi, \theta')$ . Our mode detection technique depends on obtaining one linear equation for  $A_{qn}$  (for fixed values of  $q$  and  $\psi$ ) from the Fourier transform of  $A(\psi, \theta')$  in the azimuthal direction  $\theta'$ .

2. Note that the coefficients of the unknown amplitudes  $A_{qn}$  in equation (16),  $C(m, n, \psi)k_a(m, n)$ , are known in advance and numerically given by  $q$ ,  $n$ , and  $\psi$ . These coefficients do *not* depend on experimental data. The measured data are used in finding  $D_q$  which is obtained schematically as follows

$$D_q(R_0, \alpha, V, \psi) = \text{complex const.} \times e^{-iqV\pi/2} \times \{\text{spatial F.T. [temporal F.T. of } p'(\vec{x}, t)]\} \quad (18)$$

3. In general, one must have some knowledge of  $V$  in advance. For example, if we have stator vanes, then  $V$  can be taken as the number of stator vanes. Otherwise, one can only guess about circumferentially symmetric disturbances that generate a detected mode. This is not necessarily a weakness of our method because the detected modes can guide the user to search for possible circumferential disturbances interacting with rotor blades both inside and outside the duct. For example, the ribs on an inflow control device intended to break down the atmospheric turbulence may produce wakes that can interact with rotor blades in the duct. In this case, if the ribs are placed at equal angles circumferentially,  $V$  should be taken as the number of ribs.

4. The radial wave number  $k_r(m, n)$  is found from the solution of

$$J'_m[k_r(m, n)r_0] = 0. \quad (19)$$

We index  $n$  starting with  $n = 1$  rather than  $n = 0$ . The cut-off ratio,  $\xi(m, n)$  of the mode  $(m, n)$  is given by

$$\xi(m, n) = \frac{k}{\beta k_r(m, n)} \quad (20)$$

where  $\beta = \sqrt{1 - M^2}$ . The axial wave number,  $k_a(m, n)$ , is found from

$$k_a(m, n) = \frac{k}{\beta^2} \left[ -M \pm \sqrt{1 - 1/\xi^2(m, n)} \right]. \quad (21)$$

For inlet radiation and the  $x$ -axis pointing outward, since  $M < 0$  and  $k_a(m, n) > 0$  the relation becomes

$$k_a(m, n) = \frac{k}{\beta^2} \left[ |M| + \sqrt{1 - 1/\xi^2(m, n)} \right]. \quad (22)$$

### 3. III-Posedness and Remedy

We are finding the complex amplitudes of the radiated modes  $A_{qn}$  by solving an overdetermined system of equations

$$\mathbf{G}A_q = d_q \quad (23)$$

where  $\mathbf{G}$  is a  $j \times n$  matrix,  $j \geq n$ ,  $A_q = (A_{q1}, A_{q2}, \dots, A_{qn})^T$  and  $d_q = (D_q(\psi_1), \dots, D_q(\psi_j))$ . Equation (23) is the matrix form of the system of linear equations based on equation (16) and evaluated at axial distances  $x_1, x_2, \dots, x_j$  corresponding to  $\psi = \psi_1, \psi_2, \dots, \psi_j$  such that  $\psi_1 > \psi_2 > \dots > \psi_j$ . We note that if the elements of the matrix  $\mathbf{G}$  are denoted by  $g_{vw}$ , then

$$g_{vw} = C(m, w, \psi_v)k_a(m, w) \quad (24)$$

where  $C(m, w, \psi_v)$  and  $k_a(m, w)$  are given by equations (12) and (22) with appropriate change of notation. We will show below that  $g_{vw}$  can be written in a particularly simple form which can be useful in applications. Using equation (5.54), page 634 of Gradshteyn and Ryzhik,<sup>6</sup> we have

$$C(m, w, \psi_v) = \frac{1}{\alpha_v^2 - \beta_w^2} [\beta_w r_0 J_m(\alpha_v r_0) J_{m-1}(\beta_w r_0) - \alpha_v r_0 J_{m-1}(\alpha_v r_0) J_m(\beta_w r_0)] \quad (25)$$

where

$$\alpha_v = \frac{\alpha B \Omega}{c} \sin \psi_v = k \sin \psi_v \quad (26a)$$

$$\beta_w = k_r(m, w). \quad (26b)$$

Now we use the following relation (eq. 8.472, p.967, Gradshteyn and Ryzhik<sup>6</sup>)

$$z J_m(z) = z \frac{d}{dz} J_m(z) + m J_m(z) \quad (27)$$

and the fact that  $J'_m(\beta_w r_0) = 0$ , because of the boundary condition, to simplify the right side of equation (25) and obtain

$$\begin{aligned} C(m, n, \psi_v) &= \frac{J_m(\beta_w r_0)}{\alpha_v^2 - \beta_w^2} [m J_m(\alpha_v r_0) \\ &\quad - \alpha_v r_0 J_m(\alpha_v r_0)] \\ &= \frac{J'_m(\alpha_v r_0) J_m(\beta_w r_0)}{\beta_w^2 - \alpha_v^2}. \end{aligned} \quad (28)$$

The expression on the right is not singular when  $\alpha_v \rightarrow \beta_w$  because then  $J'_m(\beta_w r_0) = 0$ . We, therefore, have

$$g_{vw} = \frac{k_a(m, n) J'_m(\alpha_v r_0) J_m(\beta_w r_0)}{\beta_w^2 - \alpha_v^2} \quad (29)$$

giving the simplest form in which  $g_{vu}$  may be written.

In general, we do not know whether a radial mode that can propagate in the duct was actually generated. Therefore, we must have the corresponding column in matrix  $\mathbf{G}$ . We propose taking more measurements in the axial direction than is necessary to find all of the radial modes. Because of measurement and numerical errors, the overdetermined system of equations (23) is not consistent. It is a good idea to keep all the linear equations and use a method to extract the amplitudes of the radiated modes from the overdetermined system of equations (23). Even with very careful measurements, it is not easy to get precise information on mode amplitude because the matrix  $\mathbf{G}$  has zero or near zero singular values and, therefore, is ill-conditioned.

To obtain a meaningful solution for  $A_q$  from equation (23), we must use a regularization technique such as singular value decomposition (SVD) or Tikhonov regularization.<sup>3,4</sup> Both methods involve first finding the  $n$  singular values  $\mu_1^2 \geq \mu_2^2 \geq \dots \geq \mu_n^2 \geq 0$  which are the eigenvalues of the  $n \times n$  matrix  $\mathbf{G}^*\mathbf{G}$ . Here,  $\mathbf{G}^*$  is the Hermitian adjoint of  $\mathbf{G}$ . It is possible that the singular values beyond some index are all zero or very small. When the singular values are very small, any errors in the elements of  $d_q$  are magnified greatly, resulting in large errors in the solution of equation (23). This situation is very common in practice, a point emphasized by Tikhonov in numerous publications.<sup>7</sup> Tikhonov suggested a regularization technique known by his name which we have used in our work.

Referring to figure 3, let  $X$  be an  $n$ -dimensional space and  $Y$  a  $j$ -dimensional space. The matrix  $\mathbf{G}$  represents a linear operator  $G : X \rightarrow Y$ . In general, the nullspace of  $G$ ,  $N_G$ , is not empty and the range,  $R_G$ , of  $G$  is not the entire space  $Y$ , i.e.,  $R_G \neq Y$ . It is entirely possible that  $d_q$  in equation (23) is not in  $R_G$ , but has a projection in  $R_G$ . We know that  $X \setminus N_G \rightarrow R_G$  is an isomorphism and, therefore,  $X \setminus N_G$  and  $R_G$  have the same dimension  $s \leq n$ . The singular values  $\mu_1, \mu_2, \dots, \mu_s$  are all non-zero. Both SVD and Tikhonov regularization depend on the construction of an orthonormal basis  $(u_1, u_2, \dots, u_s)$  in  $X \setminus N_G$  and another  $(v_1, v_2, \dots, v_s)$  in  $R_G$ . Then in the method of SVD, the solution of equation (23) is interpreted as the solution of

$$\mathbf{G}^*\mathbf{G}A_q = \mathbf{G}^*d_q \quad (30)$$

which always exists. It is given by

$$(A_q)_{\text{SVD}} = \sum_{i=1}^s \frac{1}{\mu_i} \langle d_q, v_i \rangle u_i \quad (31)$$

where  $\langle \cdot, \cdot \rangle$  is the inner product.

It is possible that some of the singular values beyond some index are very small and then small errors in  $d_q$  are magnified resulting in large errors in  $A_q$ . Tikhonov proposed to use the following result as the solution of equation (23)

$$(A_q)_T = \sum_{i=1}^s \frac{\mu_i}{\alpha_T + \mu_i^2} \langle d_q, v_i \rangle u_i \quad (32)$$

where  $\alpha_T > 0$  is a constant known as the Tikhonov parameter. This parameter is usually of the order of the square of the smallest nonzero singular values. It can be shown<sup>3</sup> that  $(A_q)_T$  minimizes the function

$$\|\mathbf{G}(A_q)_T - d_q\|_Y + \alpha_T \|(A_q)_T\|_X \quad (33)$$

which means that we are controlling the error  $\|\mathbf{G}(A_q)_T - d_q\|_Y$  and the norm of the solution  $\|(A_q)_T\|_X$ . There are many articles discussing the applications of the Tikhonov regularization method and the process of selecting the parameter  $\alpha_T$ .<sup>4</sup> We have chosen this method for the mode detection technique.

#### 4. Some Results

We now present some results from an experiment on a 16-bladed fan with 20 vanes in a duct of radius  $r_0 = 0.1524$  m (6 inches). The inlet flow Mach number was 0.605. The rotor speed was 16,900 RPM corresponding to BPF = 4507 hz. The radius of the circular microphone array was 0.912 m (3 ft.) with 18 microphones located at 10 degree intervals. The microphones rotated in steps of 0.5 degrees covering 10 degrees for a total of 360 points on the arc of half a circle. Ten axial locations were used in this test, the set-up of which is shown in figure 4.

In order to measure the phase of the complex temporal Fourier transform, a stationary reference microphone is needed to make simultaneous noise measurement with microphones on the array. The cross-spectral analysis of two microphones (reference and an array microphone) were used to get the phase information of the temporal Fourier transform. It is not at all obvious where to place the reference microphone. One would like to place the reference microphone in the peak directivity position of a mode.

This is not, in general, possible because we are looking for many modes with different directivity patterns. For this test, we have used three reference microphones at  $\psi = 30, 50, 70$  degrees, as shown in figure 4, at a constant distance of 1.83 m (6 ft) from the fan axis. Theoretically, the three reference microphones should give the same mode amplitudes for any radiated mode.

We were interested in the rotor-stator interaction modes for BPF, 2BPF, and 3BPF. The RPM of the fan rotor was varying within 0.6 percent of the specified value. For modes that radiate outside the duct, (*i.e.* the modes that are not very close to cut-off), we should be able to find their amplitudes with this small variation in RPM. The reason is apparent from equation (17). The temporal Fourier transform of  $p'(\vec{x}, t)$  gives a complex quantity independent of  $\Omega$ . Thus, small variations in  $\Omega$  should not introduce errors in the amplitudes of the radiated modes.

### Test Results

1. The phase of the temporal complex Fourier transform is always given relative to the reference microphone. Therefore, for a fixed axial location of the array and over the 360 microphone positions on the half-circle, the phase distributions from two reference microphones should show a constant shift between them. This is a good test of the phase measurement technique and instrumentation. For BPF and 2BPF, the shift varied by approximately 5 degrees. For 3BPF, the shift variation was larger at approximately 10 degrees. This order of accuracy does not seem to be satisfactory. This can be a source of error in finding the mode amplitudes and the disagreement of the results from different reference microphones.

2. The following are the possible interaction modes that can radiate noise outside the inlet:

**BPF:** (-4,1) to (-4,3)

**2BPF:** (-28,1), (-8,1) to (-8,7), (12,1) to (12,5)

**3BPF:** (-32,1) to (-32,3), (-12,1) to (-12,10), (8,1) to (8,12), (28,1) to (28,4)

We will present results for some of the modes shown here. Since we had 10 axial stations in the test, we cannot compute the amplitudes of modes (8,11) and (8,12) for 3BPF.

3. Ill-posedness of the problem becomes obvious if we look at the singular values of the matrix  $\mathbf{G}$  (square roots of the eigenvalues of  $\mathbf{G}^*\mathbf{G}$ ). For circumferential mode -12 at 3BPF, these are:

$n$	$\mu_i$
1	4.42e-4
2	3.63e-4
3	2.98e-4
4	2.37e-4
5	2.10e-4
6	1.73e-4
7	5.58e-5
8	9.89e-7
9	3.44e-9
10	1.52e-12

Table 1. Singular values for radial modes of  $m = -12$  at 3BPF

It is quite obvious that we have a very ill-conditioned matrix  $\mathbf{G}^*\mathbf{G}$ . Similar behavior has been observed for other modes. This is a clear indication of the ill-posedness of the mode detection problem.

The general rule for using a regularization technique is that one must have a good idea about the errors in equation (23). In our case, we must be concerned with errors in the measured quantity,  $d_q$ , because the elements of  $\mathbf{G}$  are known analytically to machine accuracy. A phase error of  $\Delta\phi$  in the temporal Fourier transform introduces an error in  $d_q$  that is magnified when finding the mode amplitude by a factor  $1/\mu_i$  if the error vector lies along the basis vector,  $v_i$ , in  $Y$  space (see equation (31)). Because the singular value  $\mu_i$  can be very small, the error introduced in the computed mode amplitude can be relatively large.

After testing various values of the Tikhonov parameter,  $\alpha_T$ , it was decided that a value of  $\alpha_T = 10^{-10}$  was a good choice, essentially affecting  $\mu_i \approx 10^{-5}$  and smaller. The following results have been calculated using this value of the Tikhonov parameter.

4. Mode amplitudes for BPF from the three reference microphones are shown in figure 5. In this figure, and those following, we will not show the amplitude of the radial mode nearest to cut-off (highest radial mode) unless there is only one mode that is cut on. Figure 5 shows the good agreement between

the three reference microphones in determining the mode amplitudes.

Figure 6 shows amplitudes of the radiated modes for 2BPF and figure 7 shows similar results for 3BPF. In both of these figures, we see that there are some large amplitudes for modes near cut-off. Because these modes have predominantly in-plane directivity, these large amplitudes are almost definitely caused by the ill-conditioning problem of the matrix  $\mathbf{G}$ . Otherwise, there is general agreement between the amplitudes of the modes computed from the three reference microphones, although there are some notable disagreements. It appears that errors in the phase measurements of the temporal Fourier transform of  $p'(\vec{x}, t)$  are the main cause of the discrepancies.

On the whole, we can claim that the mode detection technique discussed in this paper appears to be doing a good job of giving us the mode amplitudes. Further refinements of the technique are possible as discussed below.

### 5. Concluding Remarks

We have presented a mode detection theory for noise radiated from the inlet or the exhaust of an engine. We have shown that the spatial Fourier transform in the azimuthal direction of the complex temporal Fourier transform of the acoustic pressure  $p'(\vec{x}, t)$  has the information about the amplitudes of all the modes radiated outside of the duct. The problem of mode detection is ill-posed and a regularization technique such as SVD or the Tikhonov method must be used to obtain meaningful results. In using any regularization technique, one must have an estimate of the errors in the measured quantities used as input to the linear system whose solution gives the amplitudes of the radiated modes. This estimate is not always available resulting in some loss of accuracy.

The example given in this paper shows that our mode detection technique is capable of finding the amplitudes of the radiated modes. It can be a very useful tool in the control and reduction of engine noise. There are many areas of improvement to make this method more useful such as:

- i. Improving the accuracy of phase measurements of the complex temporal Fourier transform of the noise at microphone locations.

- ii. Changing the duct radiation model to include the effect of refraction of sound by the inflow or exhaust stream. This will complicate the algebra for setting up the linear system of equation (23), but will undoubtedly be a more realistic model than the one currently employed.
- iii. Exploring other regularization techniques.<sup>3,4</sup> Currently, many problems of science and technology are ill-posed and many publications address the selection of the regularization method. Some of these are good candidates for the mode detection problem.

### Acknowledgments

The authors thank Carl Gerhold, Lorenzo Clark, Florence Hutcheson, Jeff Kelly, and Larry Becker for help in design, testing, and data analysis. The authors are grateful to Larry Heidelberg of Glenn Research Center for his assistance on the literature of mode detection.

### References

1. Pickett, G.F., Sofrin, T.G., and Wells, R.A., "Method of Fan Sound Mode Structure Determination. Final Report," NASA CR-135293, Aug. 1977.
2. Heidelberg, L.J. and Hall, D.G., "Inlet Acoustic Mode Measurements Using a Continuously Rotating Rake," *Journal of Aircraft*, Vol. 32, No. 4, 1995, pp.761-767.
3. Kress, Rainer, *Numerical Analysis*, Springer-Verlag, 1998, Chapter 5.
4. Engl, Heinz W., Hanke, Martin, Neubauer, Andrea, *Regularization of Inverse Problems*, Kluwer Academic Publishers, 1996, Chapter 5.
5. Farassat, F. and Myers, M.K., "A Study of Wave Propagation in a Duct and Mode Radiation," May 6-8, 1996, State College, PA, AIAA/CEAS Paper No. 96-1677.
6. Gradshteyn, I.S. and Ryzhik, I.M., *Tables of Integrals, Series, and Products*, 4th Ed., Academic Press, 1965.
7. Tikhonov, A.N. and Arsenin, V., *Solutions of Ill-Posed Problems*, Wiley, 1977.

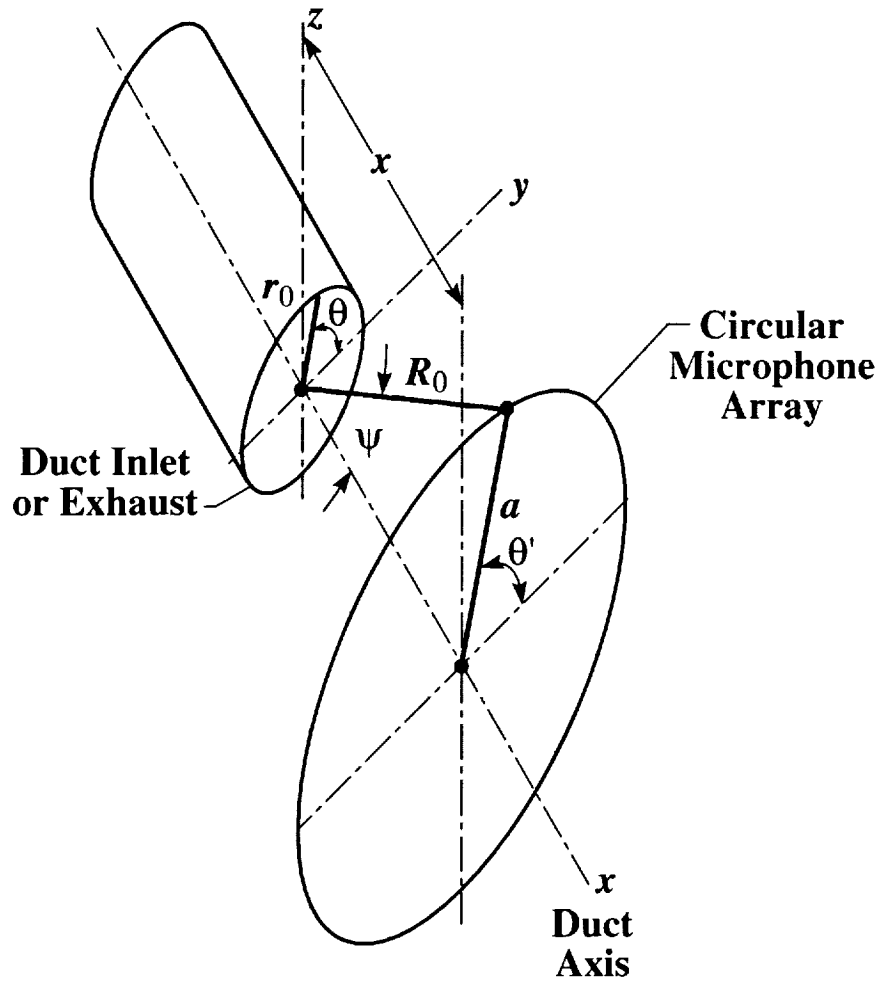


Figure 1. Microphone array and duct geometry

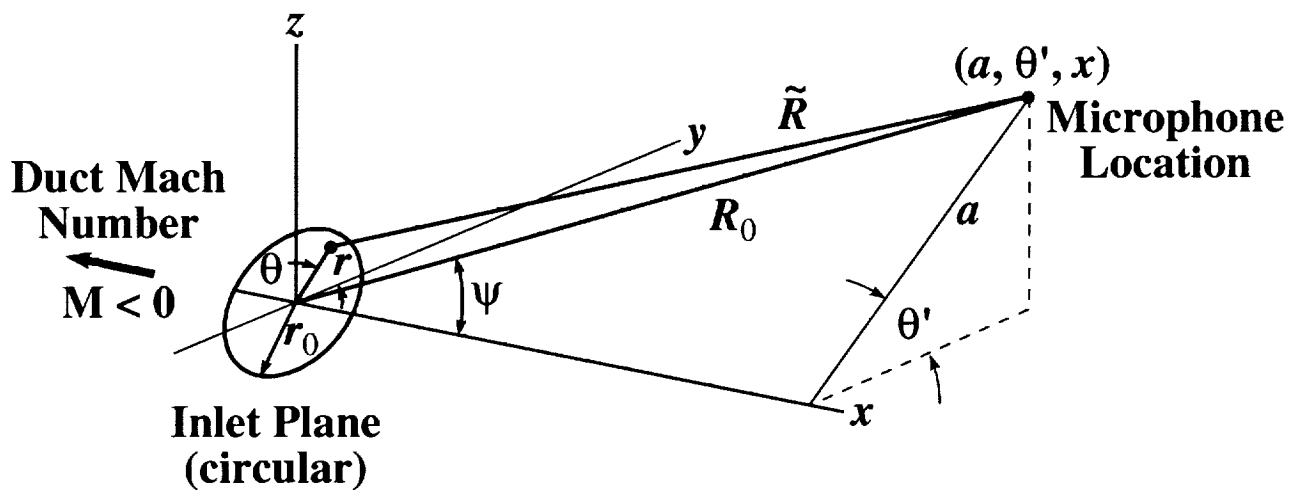


Figure 2. Description of symbols used for mode detection theory



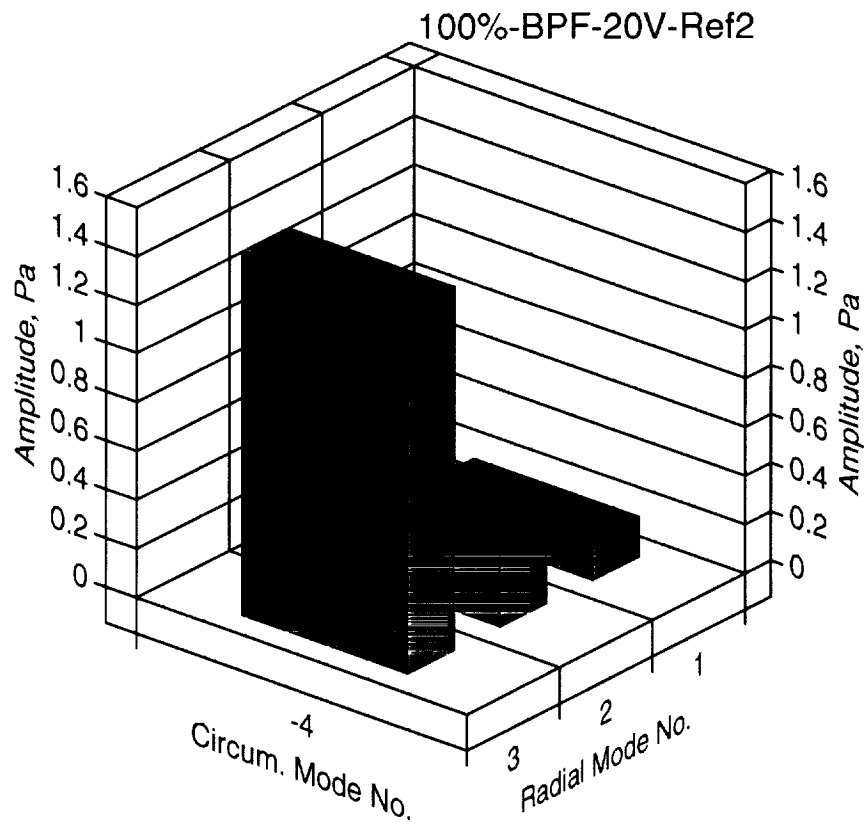
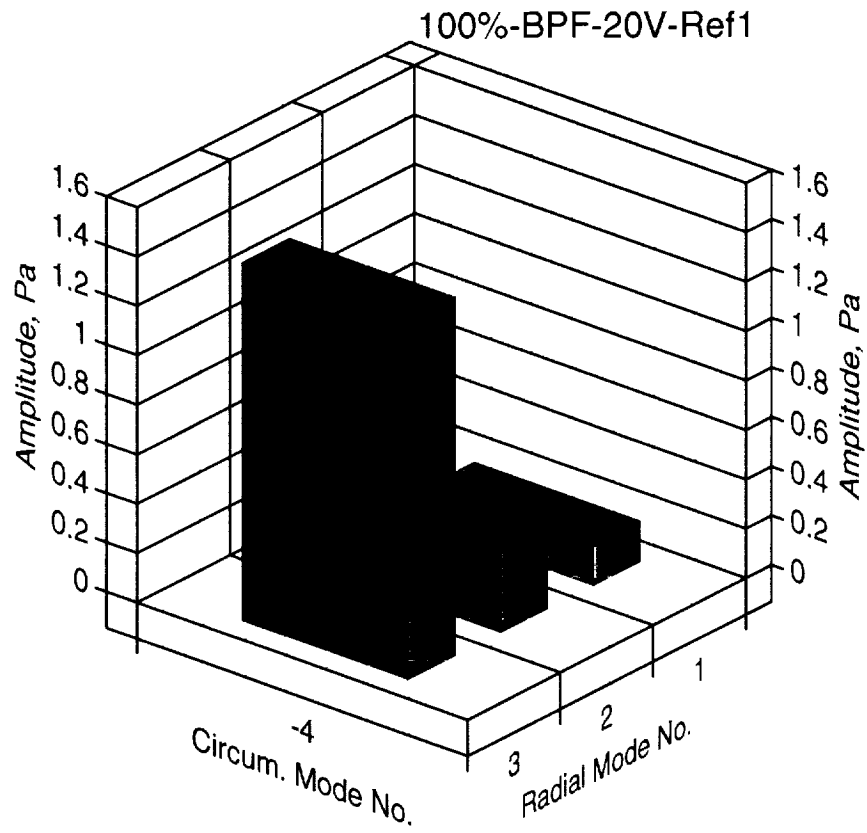


Figure 5. Radial Mode Amplitudes for BPF using the three reference microphones

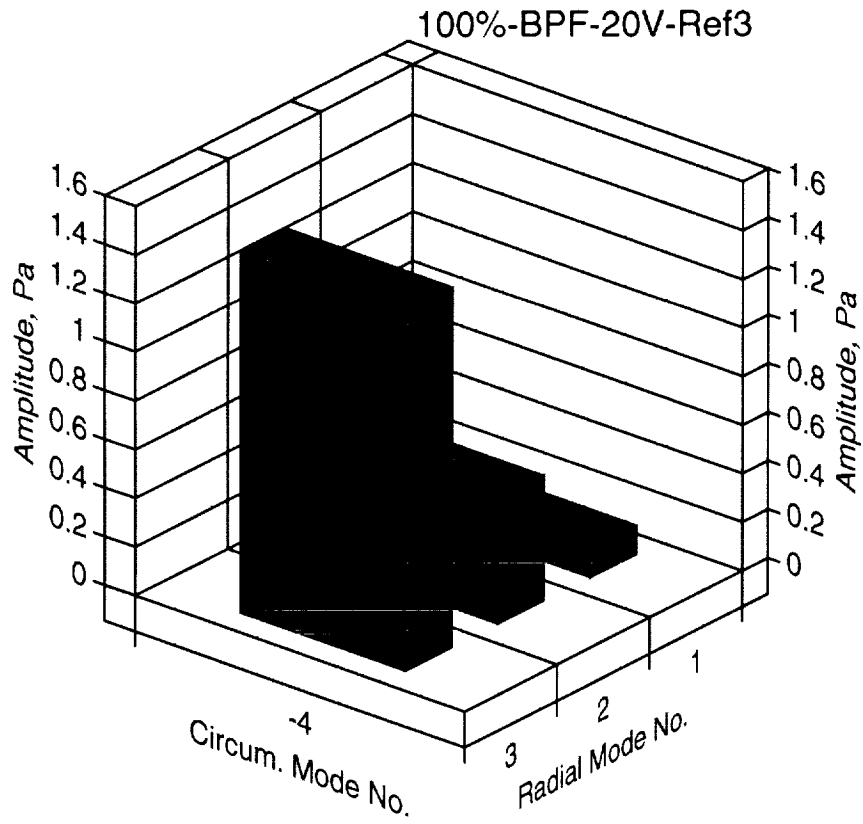


Figure 5. Radial Mode Amplitudes for BPF using the three reference microphones (cont.)

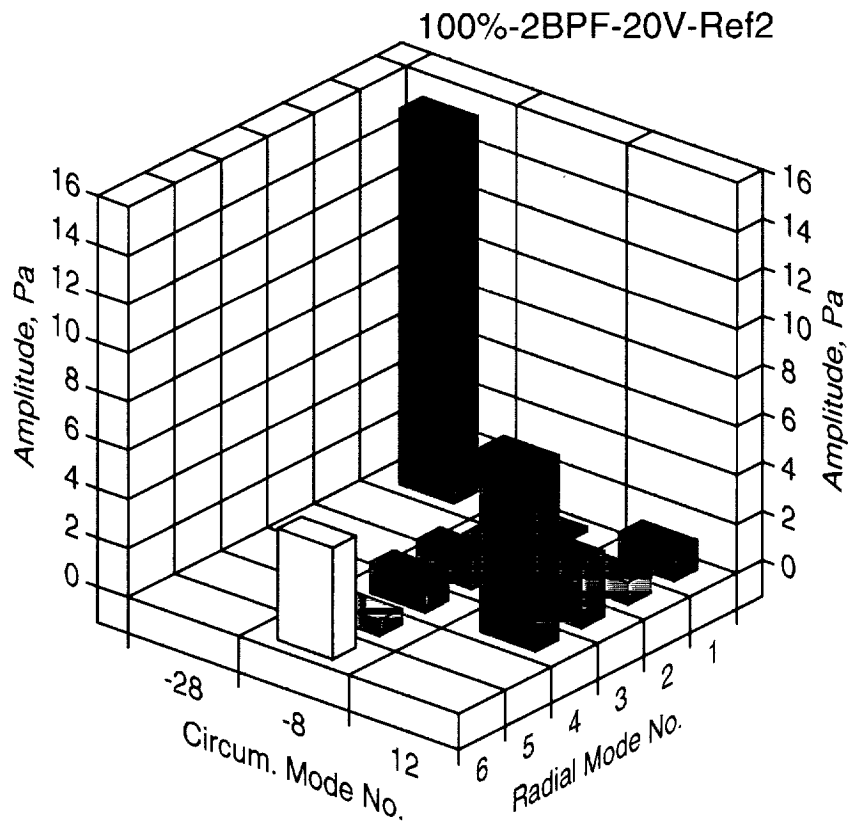
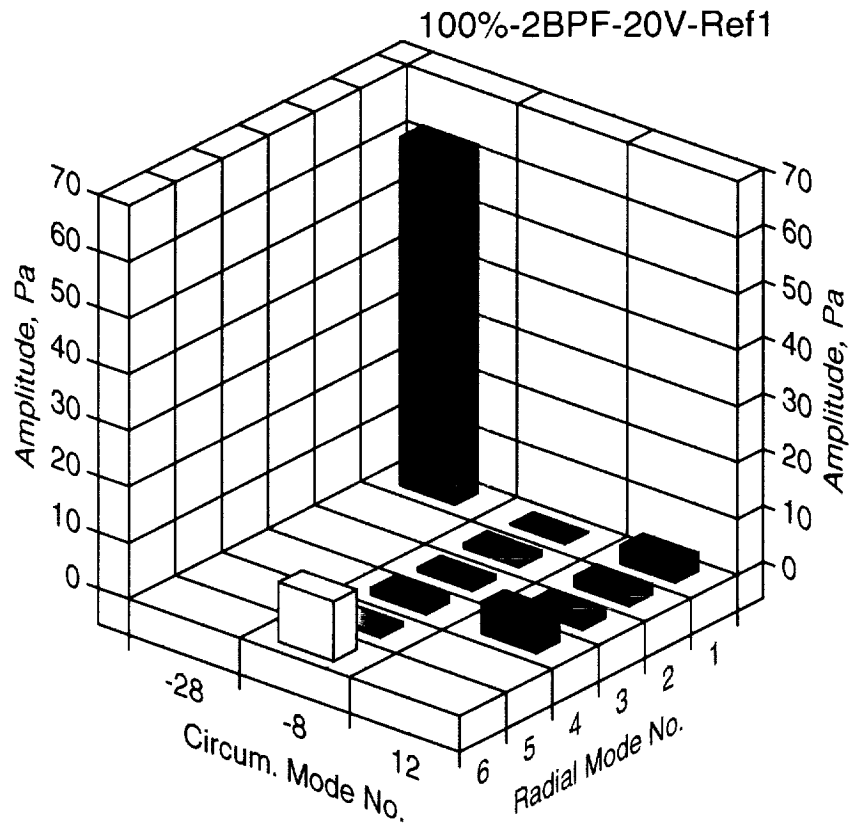


Figure 6. Radial Mode Amplitudes for 2BPF using the three reference microphones

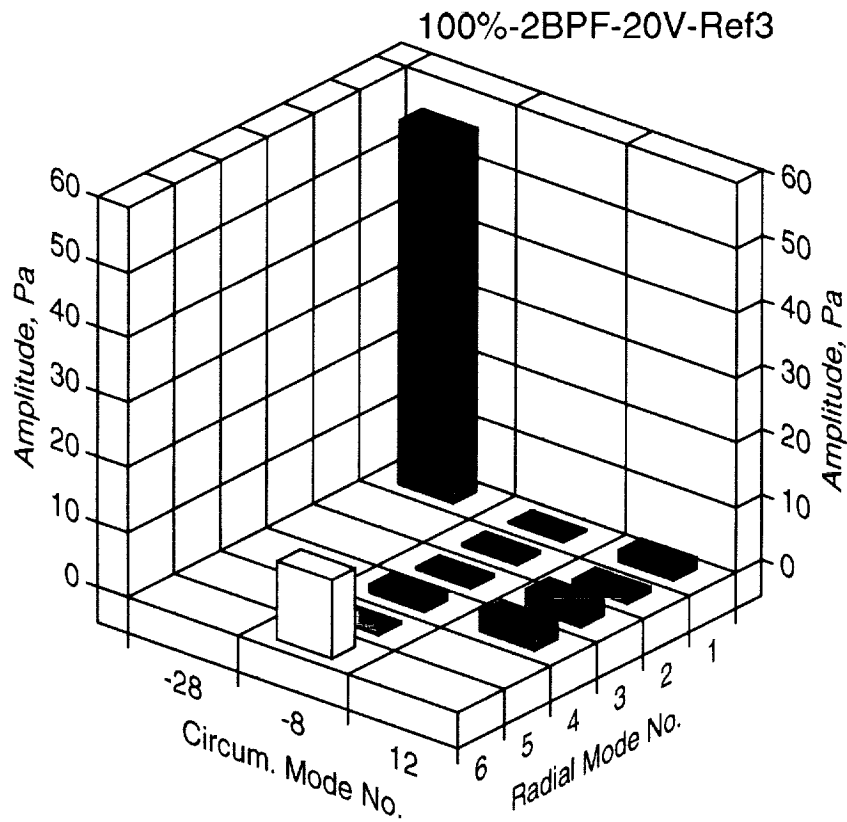


Figure 6. Radial Mode Amplitudes for 2BPF using the three reference microphones (cont.)

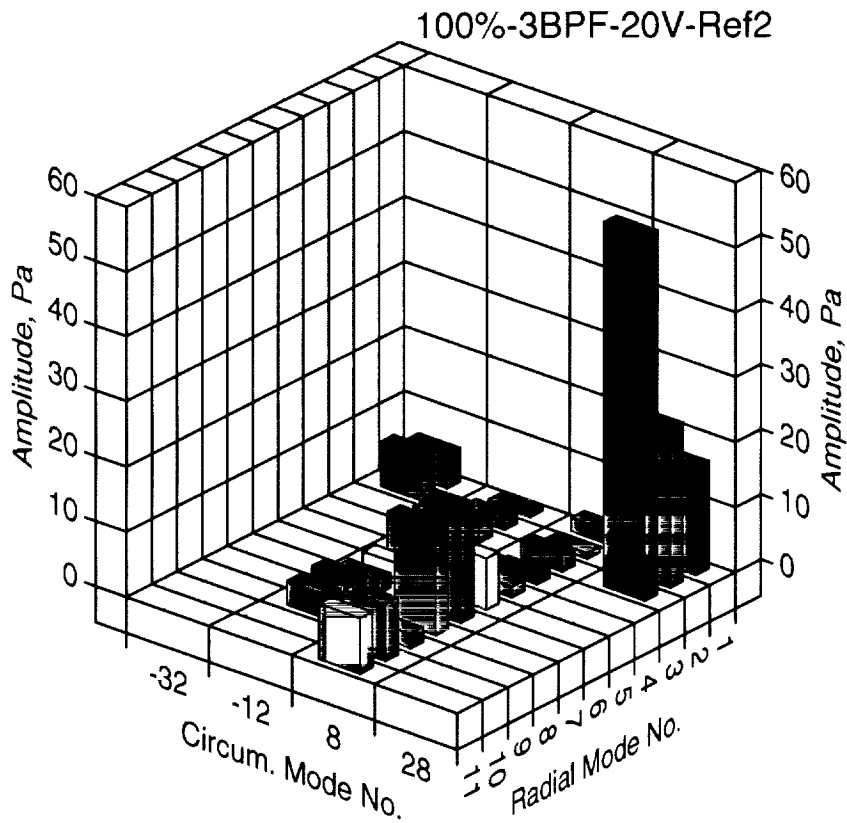
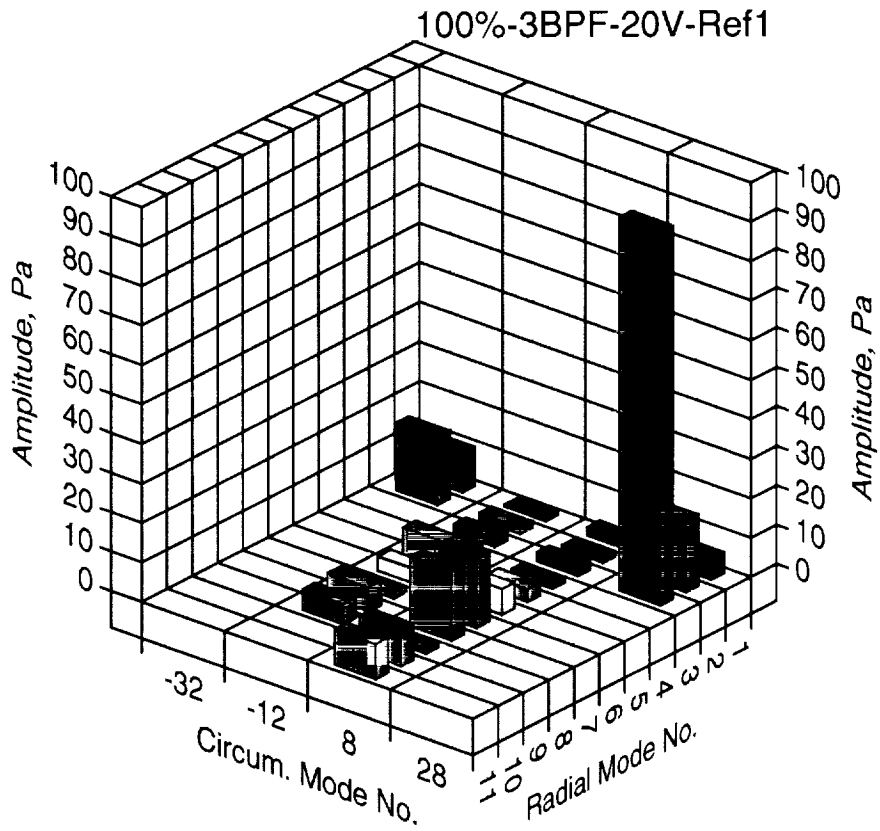


Figure 7. Radial Mode Amplitudes for 3BPF using the three reference microphones

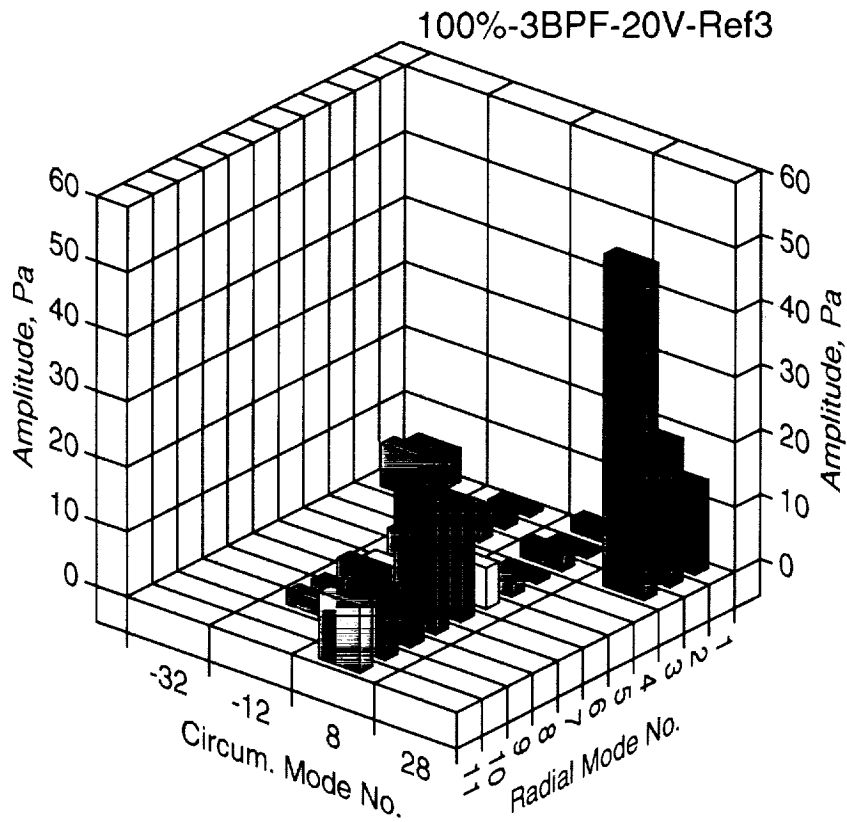


Figure 7. Radial Mode Amplitudes for 3BPF using the three reference microphones (cont.)